CORE
Metadata, citation and similar papers at core.ac.uk
Provided by University of Bath Research Portal

Citation for published version:
Regan, EM, Hallett, AJ, Wong, LCC, Saeed, IQ, Langdon-Jones, EE, Buurma, NJ, Pope, SJA & Estrela, P 2014, 'A novel cobalt complex for enhancing amperometric and impedimetric DNA detection', Electrochimica Acta, vol. 128, pp. 10-15. https://doi.org/10.1016/j.electacta.2013.10.028

DOI:
10.1016/j.electacta.2013.10.028

Publication date:
2014

Document Version
Peer reviewed version

Link to publication

NOTICE: this is the author's version of a work that was accepted for publication in Electrochimica Acta. Changes resulting from the publishing process, such as peer review, editing, corrections, structural formatting, and other quality control mechanisms may not be reflected in this document. Changes may have been made to this work since it was submitted for publication. A definitive version was subsequently published in Electrochimica Acta, V.128. May 2014.
DOI: 10.1016/j.electacta.2013.10.028

University of Bath

General rights
Copyright and moral rights for the publications made accessible in the public portal are retained by the authors and/or other copyright owners and it is a condition of accessing publications that users recognise and abide by the legal requirements associated with these rights.

Take down policy
If you believe that this document breaches copyright please contact us providing details, and we will remove access to the work immediately and investigate your claim.

Download date: 13. May. 2019

A novel cobalt complex for enhancing amperometric and impedimetric DNA detection

Edward M. Regan[a], Andrew J. Hallett[b], L. C. Caleb Wong[a], Ibrahim Q. Saeed[b], Emily E. Langdon-Jones[b], Niklaas J. Buurma[b], Simon J. A. Pope[b], Pedro Estrela[a,1]

[a] Department of Electronic & Electrical Engineering, University of Bath, Bath BA2 7AY, United Kingdom.

[b] School of Chemistry, Cardiff University, Park Place, Cardiff CF10 3AT, United Kingdom.

[1] ISE Member

Corresponding author: Dr Pedro Estrela

Dept. Electronic & Electrical Engineering, University of Bath

Bath BA2 7AY, United Kingdom.

E-mail: p.estrela@bath.ac.uk

Phone: +44-1225-386324

ABSTRACT

In this work we present a novel cobalt complex, $[Co(GA)_2(aqphen)]Cl$ that is water-soluble, redox-active and binds to dsDNA. We report that this complex can be used as a signal enhancer when detecting DNA hybridisation using electrochemical impedance spectroscopy (EIS) and differential pulse voltammetry (DPV). The compound mediates its EIS signal enhancement by causing an increase in charge transfer resistance (R_{ct}) when bound to dsDNA. Increased peak currents are also observed with DPV when the compound is incubated with dsDNA as compared with ssDNA. We believe that this compound intercalates specifically with dsDNA and alters the DNA structure to affect the electrostatic barrier to charged redox markers in solution. To our knowledge this is the first example of a single compound that can enhance both amperometric and impedimetric signals for DNA detection. Our findings enable the development of a label-free and multi-modal approach to improve the sensitivity, accuracy and speed of electrochemical DNA detection.

Keywords: DNA sensors; intercalators; electrochemical impedance spectroscopy; differential pulse voltammetry

1. Introduction

Techniques for detecting nucleic acid sequences have numerous clinical, ecological and forensic applications. These include identifying genetic disorders and diseases (e.g. cancer), the presence of pathogenic microbes and the determination of biological contaminants in food and water [1,2]. Optical systems that utilise micro-array technology, fluorescent probes and/or the polymerase-chain reaction (PCR) are typically used for nucleic acid detection but can be expensive and time consuming [3]. Electrochemical nucleic acid sensors (genosensors) have been shown to provide sensitive and inexpensive nucleic acid detection from complex samples, without the need for target purification and require a reduced number of PCR-based amplification steps [1,4]. In addition, these systems can be engineered for low power requirements and miniaturization, making them a suitable platform for providing a portable tool for point-of-care testing [2].

Electrochemical nucleic acid sensors couple the molecular recognition of sequence hybridisation directly to a transducer that produces a measurable signal. Multiple electrochemical modes of detection exist that include amperometric (e.g. cyclic voltammetry, differential pulse voltammetry) and impedimetric (e.g. impedance spectroscopy) techniques that monitor changes in current, resistance or impedance following the binding of target sequences. To mediate a measurable change after target binding these modes can use either (1) direct detection of hybridisation (label-free), (2) labelling of the target nucleic acid sequences with redox active substances/nanoparticles or (3) signal probes (indirect labels) that intercalate within the stacked base pairs, electrostatically bind to the phosphate backbone or sit within the grooves of the double helix [2,5]. Whilst label-free methods are often desirable for having fewer sample processing steps, they generally do not display the same levels of sensitivity as labelled methods. Indirect labels like intercalating molecules can offer

a useful compromise between easier sample preparation and improved detection sensitivity, whereby direct labelling of the target nucleic acid sequence is not required.

Various types of intercalating molecules have been used to provide signals to detect DNA hybridisation, typically using cyclic voltammetry (CV) or differential pulse voltammetry (DPV). These intercalators are usually cationic metal complexes, anti-cancer drugs (e.g. epirubicin, mitoxantrone), antibiotics (e.g. daunomycin) or other redox-active molecules (e.g. methylene blue) [6-11]. Many types of cationic metal complexes have been tested that use Co(III), Ru(II), Fe(II), Os(II/IV) chelates with relatively simple commercially available ligands like 1,10-phenanthroline (phen) and 2,2′-bipyridine [12-16]. These substances provide reversible redox probes that interact in a different way with ssDNA and dsDNA and so allow the level of dsDNA to be measured. Previous studies have applied cationic metal complexes to investigate interactions between DNA and antioxidants [17], for the detection of hepatitis B virus DNA [8,18] and calf thymus DNA as well as other polynucleotides [13,14,16]. Furthermore, metal ion complexes can be modified by altering the chelating component so that properties such as binding affinity, solubility and chemical stability can be optimised.

In addition to enhancing detection for amperometric methods, different enhancement mechanisms also exist for impedimetric detection that can improve nucleic acid detection. A variety of techniques have been demonstrated for increasing sensitivity to DNA hybridisation detection by amplifying changes in charge transfer resistance (R_{ct}). These methods include forming surface precipitants by enzymatic linkages to DNA [19] and binding gold nanoparticles, quantum dots or carbon nanotubes to the electrode surface [2]. Some of these amplification methods have allowed nucleic acid detection in the attomolar range without the need for PCR. DNA intercalators, e.g. $[Ru(phen)_3]^{2+}$, spermine, actinomycin D, proflavine have also been used in conjunction with EIS to serve as signal validation tools to exclude

potential false positives by non-specific adsorption [20,21]. These molecules cause a decrease in R_{ct} upon binding to dsDNA, but cause little or no change with ssDNA. To our knowledge, cationic metal complexes molecules have not been used to enhance DNA detection sensitivity by increasing R_{ct} using electrical impedance spectroscopy (EIS).

We have focussed our study on the use of a cobalt complex that we have modified from a substance highlighted in a study by Lin *et al.* [22]. The complex used by Lin *et al*. contained a mixed-ligand coordination sphere of 1,10-phenanthroline (phen) and glycolic acid (GA); $[Co(GA)_2(phen)]$ was demonstrated to bind to dsDNA, most likely in the intercalative mode. In the present study, this complex has been modified to contain an extended planar ligand (aqphen = naphtho[2,3-*a*]dipyrido[3,2-*h*:2′,3′-*f*]phenazine-5,18-dione) [23] with a conjugated anthraquinone unit, that we have shown to improve the binding affinity of the complex to dsDNA. Furthermore, we show how it is possible to use this molecule both as a sensitive redox-probe and as an enhancer for impedimetric (EIS) detection of DNA hybridisation. We believe that this is the first example of multi-modal applications using a metal complex that can simultaneously enhance amperometric and impedimetric DNA detection without the need for multi-step amplification techniques such as enzymatic reactions.

2. Experimental

2.1. Materials

Thiol-modified and non-modified DNA oligonucleotides were purchased from Sigma Aldrich (HPLC purified). 6-Mercapto-1-hexanol (97%), potassium phosphate monobasic solution (1 M), potassium phosphate dibasic solution (1 M), potassium sulphate, potassium hexacyanoferrate (III), potassium hexacyanoferrate(II) trihydrate, ethylenediaminetetraacetic acid (EDTA, 0.5 M) and magnesium chloride were all purchased from Sigma-Aldrich.

$CoCl_2.6H_2O$, 1,10-phenanthroline monohydrate and 1,2-diaminoanthraquinone were all used as purchased from Alfa Aesar. All synthesis reactions were performed with the use of vacuum line and Schlenk techniques. All aqueous solutions were prepared using 18.2 MΩ cm ultra-pure water (Millipore, Billerica, MA, USA) with a Pyrogard filter (Millipore) to remove nucleases.

2.2. Synthesis of $[Co(GA)_2(aqphen)]Cl$

Under a nitrogen atmosphere, $CoCl_2.6H_2O$ (0.137 g, 0.576 mmol) was dissolved in ethanol (10 mL) and mixed with naphtho[2,3-*a*]dipyrido[3,2-*h*:2′,3′-*f*]phenazine-5,18-dione (aqphen) (0.237 g, 0.576 mmol) for 30 min. Then, an ethanol/water (95:5) solution (10 mL) of glycolic acid (0.090 g, 1.183 mmol) neutralized by KOH (0.066 g, 1.176 mmol) was added and the mixture stirred for 1 h. The resulting orange precipitate was filtered and dried *in vacuum*. Elemental analysis: Calcd. (%) for $C_{30}H_{20}N_4CoO_9Cl$: C, 53.39, H, 2.99, N, 8.30; Found: C, 53.67, H, 2.36, N, 7.86. ES MS found *m/z* 546.0, calculated *m/z* 546.0 for $[M\text{-}C_2H_3O_3]^+$. HR MS found *m/z* 546.0366, calculated *m/z* 546.0369 for $[C_{28}H_{15}CoN_4O_5]^+$. UV-vis (DMSO): λ_{max} (ε / dm^3 mol^{-1} cm^{-1}) 282 (14650), 405 (3850) nm.

Aqueous stock solutions containing 1 mM $[Co(GA)_2(aqphen)]Cl$ were prepared by dissolving the required amount of the complex in water by heating or by heating to 70 °C in a sonicator bath for one hour.

2.3. General analysis

High-resolution mass spectra were carried out at the EPSRC National Mass Spectrometry Service at Swansea University. UV-Vis studies were performed on a Jasco V-570

spectrophotometer as a DMSO solution (4.2×10^{-5} M). Microanalysis was performed at the London Metropolitan University.

Docking studies were carried out using Autodock Vina 1.1.2 [24]. The required PDBQT files for low-spin and high-spin $Co(GA)_2(aqphen)$ were generated using AutoDockTools 1.5.6 rc3 [25] from DFT-optimized structures. The structures for $Co(GA)_2(aqphen)$ were kept rigid. The construction of the PDBQT file for the rigid target DNA structure displaying a pre-formed intercalation gap was described previously [26]. The grid box dimensions are 40 × 40 × 60 Å. Docked poses were visualized using UCSF Chimera [27].

DFT structure optimizations for both the low-spin and high spin forms of $Co(GA)_2(aqphen)$ were carried out using GAMESS-US [28] (version of 11 August 2011), employing the Minnesota M06 functional [29], and the 6-31(p,d) basis set for all atoms. Optimizations were carried out using both UHF and ROHF methods. Structures were optimized to (local) minima without constraints. The gradient convergence criterion (OPTTOL) was set to the default value of 0.0001.

2.4. Electrochemical measurements

Cyclic voltammetry on the cobalt complex was carried out using a Parstat 2273 potentiostat in conjunction with a three-electrode cell. The auxiliary electrode was a platinum wire and the working electrode a platinum (1.0 mm diameter) disc. The reference was a silver wire separated from the test solution by a fine porosity frit and an agar bridge saturated with KCl. The $[Co(GA)_2(aqphen)]Cl$ solutions were made at a concentration of 1.0×10^{-3} mol dm^{-3} in dimethylformamide (10 ml) and contained 0.1 mol dm^{-3} $[NBu^n_4][PF_6]$ as the supporting electrolyte. Under these conditions, E^0, for the one-electron oxidation of $[Fe(\eta\text{-}C_5H_5)_2]$ added to the test solutions as an internal calibrant, is +0.45 V in dimethylformamide. Unless specified, all electrochemical values are at υ = 200 mV s^{-1}.

Electrochemical Impedance spectroscopy and differential pulse voltammetry measurements were performed using an μAutoLab Type III FRA2 potentiostat (Metrohm, UK). A conventional 3-electrode configuration was used consisting of a 1.0 mm radius gold disk working electrode (CH Instruments, Austin, TX, USA), a platinum wire counter electrode (ALS instruments) and a Hg/Hg_2SO_4 (K_2SO_4 sat.) reference electrode (BASi, USA) placed into a salt bridge and against which all potentials are quoted.

The electrochemical impedance spectrum was measured in a solution of 2 mM $K_4[Fe(CN)_6]$ + 2 mM $K_3[Fe(CN)_6]$ in 50 mM phosphate buffer (PB) + 100 mM K_2SO_4 pH 7.0, ionic strength 447 mM. The reference electrode was connected via a salt bridge filled with 50 mM PB + 100 mM K_2SO_4 pH 7.0. The impedance spectrum was measured over the frequency range 100 kHz to 100 mHz, with a 10 mV a.c. voltage superimposed on a d.c. bias of −0.195 V, which corresponds to the formal potential of the redox couple.

For the differential pulse voltammetry (DPV) measurements, electrodes were placed in 100 mM PB and the DPV scans run between -0.7 V and -0.3 V vs Hg/Hg_2SO_4 (scan rate 0.05 V/s, step potential 0.005 V, modulation amplitude 0.05 V, modulation time 0.05 s, interval time 0.1 s).

2.5. Preparation of the DNA self-assembled monolayer (SAM)

Gold disk working electrodes with a radius of 1.0 mm (CH Instruments, Austin, TX,USA) were polished with 50 nm aluminium oxide particles (Buehler, Lake Bluff, IL, USA) on a polishing pad (Buehler), followed by sonication in water, polishing on a blank polishing pad, and sonication in water to remove any particles. Electrodes were subsequently electrochemically cleaned in 0.5 M H_2SO_4 by scanning the potential between the oxidation and reduction of gold, −0.05 V and +1.1 V versus an Hg/Hg_2SO_4 reference electrode, for 60

cycles until there was no further change in the voltammogram. Electrodes were rinsed with deionised water, dried in a stream of nitrogen, and exposed to 150 μL of mixed DNA/MCH immobilization solution for 16 h in a humidity chamber. Probe ssDNA had the 21-base sequence AGA AGA AGA AGA AGA AGA AGA and was modified on the 5' end to give HS-$(CH_2)_6$–ssDNA. The DNA immobilization buffer consisted of 0.8 M phosphate buffer (PB) + 1.0 M NaCl + 5 mM $MgCl_2$ + 1 mM ethylene diamine tetraacetic acid (EDTA) pH 7.0. After immobilization, electrodes were rinsed in 50 mM PB + 100 mM K_2SO_4 + 10 mM EDTA (pH 7.0) to remove any remaining Mg^{2+}. To ensure complete thiol coverage of the gold surface, the electrodes were backfilled with mercaptohexanol (MCH) by immersion in 1 mM MCH in ultra-pure water for 1 h. Electrodes were then rinsed with ultra-pure water and placed in to 50 mM PB + 100 mM K_2SO_4 pH 7.0 for 1 h.

2.6. DNA hybridisation and $[Co(GA)_2(aqphen)]Cl$ incubation

Electrodes with immobilised DNA/MCH were treated with DNA that had a complementary binding sequence to the probe DNA (5'-TCT TCT TCT TCT TCT TCT TCT-3'). Electrodes were incubated in 150 μL complementary DNA (1 μM) diluted in 50 mM PB + 100 mM K_2SO_4 pH 7.0 for 45 minutes. Electrodes were then rinsed in 50 mM phosphate buffer (PB) + 100 mM K_2SO_4 pH 7.0 buffer.

After DNA hybridisation and further EIS measurements, the electrodes were incubated in a mixture containing 200 μM $[Co(GA)_2(aqphen)]Cl$ for 30 minutes (the $[Co(GA)_2(aqphen)]Cl$ in H_2O stock solution was mixed 1:2 with 50 mM PB + 100 mM K_2SO_4 pH 7.0 buffer) . Following incubation, electrodes were rinsed in 50 mM PB + 100 mM K_2SO_4 pH 7.0 buffer and EIS/DPV measurements were made.

2.7. DNA affinity studies

Fish sperm (FS DNA) DNA was from Acros and was dialysed (MWCO 3.5 kDa) against deionised water before use. DNA concentrations, in terms of base pairs, in stock solutions were determined using the extinction coefficient of FS DNA (ε_{260nm} = 12800 M^{-1} cm^{-1}). For the DNA affinity studies, a concentrated stock solution of $Co(GA)_2$(aqphen) was diluted to the desired concentration and placed in a 1 cm pathlength cuvette thermostated at 25 °C. Aliquots of a concentrated solution of fish sperm DNA were added. After every addition, UV-visible spectra were recorded over the range 200-600 nm using an Applied Photophysics Chirascan spectropolarimeter coupled to a Julabo AWC100 water bath acting as a stable heat sink or a JASCO V630 UV-visible spectrophotometer with a Peltier thermostating unit. Titrations curves were extracted from the data and the second of the data was analysed in terms of a multiple independent (but identical) binding site type model, correcting for $Co(GA)_2$(aqphen) dilution.

3. Results and Discussion

3.1. Synthesis of [$Co(GA)_2$(aqphen)]Cl

The synthesis of the ligand was achieved using an adapted literature procedure from Lopez *et al.* [23], wherein 1,2-diaminoanthraquinone was condensed with 1,10-phenanthroline-5,6-dione to give the desired ligand. The target cobalt complex (Fig. 1), which incorporates glycolic acid co-ligands for enhanced water solubility, was synthesised using the procedure described by Lin *et al.* [22], isolating the mixed ligand species as an orange solid. The characterisation of the complex [$Co(GA)_2$(aqphen)]Cl was achieved using UV-vis spectroscopy, mass spectrometry and elemental analyses, all of which were consistent with the formulation, suggesting that the cobalt is oxidised during the reaction.

[Figure 1]

3.2. Docking studies

Based on its structure, $Co(GA)_2(aqphen)$ is expected to interact with DNA by intercalation between the basepairs. To explore the feasibility of this binding mode, a molecular docking study was carried out using AutoDock Vina [24]. Our previously developed [26] DNA structure displaying a pre-formed intercalation gap, open-d(ATCGAGA**CG**TCTCGAT)$_2$, was used as the biomacromolecular target. Structures for the complex were optimized using density functional theory (DFT) using the M06 functional. Because cobalt can form both low-spin and high-spin octahedral complexes, structures for both spin states were optimized. Although our calculations suggest that the high-spin state is most stable, DFT is known to be poor in reproducing energy differences between spin states [30]. Docking studies were therefore carried out for both of the resulting structures.

The top poses (Figure 2) all correspond to an intercalative binding mode, as anticipated.

[Figure 2]

3.3. Cyclic Voltammetry of $[Co(GA)_2(aqphen)]Cl$

The cyclic voltammetry recorded in deaerated DMF (scan rate ν = 200 mVs^{-1}, NBu_4PF_6 as supporting electrolyte) shows three reduction waves at -0.45, -0.93 and -1.47 V *versus* NHE (Fig. 3). The aqphen ligand is known to possess two one-electron reductions (to the semi-quinone and diol, respectively) [31] and therefore the most easily accessible reduction was attributed to the Co(III)/Co(II) couple.

[Figure 3]

3.4. DNA-[Co(GA)$_2$(aqphen)]Cl complex binding affinity study

The affinity of Co(GA)$_2$(aqphen) for double-stranded DNA was explored using UV-visible titrations in deionised water. The results of representative titrations are shown in Fig. 4. The titrations show two separate events. The first binding event is complete upon the addition of only 10 μM DNA (the binding constant for this event is therefore > 10^6 M^{-1}) and involves precipitation of the resulting complex as suggested by the increase scattering as quantified by the absorbance between 550 and 600 nm, where neither the complex nor the DNA absorbs. Analysis of the data for the second event in terms of the multiple independent binding sites model gives an apparent affinity of Co(GA)$_2$(aqphen) for double-stranded DNA to be in the order of 10^5 M^{-1} and a binding site size of two to three base pairs.

[Figure 4]

3.5. Impedimetric responses to the [Co(GA)$_2$(aqphen)]Cl complex

The ability of the [Co(GA)$_2$(aqphen)]Cl complex to enhance impedimetric DNA hybridisation detection was assessed using EIS. Self-assembled monolayers (SAMs) were formed on gold by co-immobilisation of thiolated oligonucleotides and mercaptohexanol (MCH), as previously described by Keighley *et al.* [32]. The charge transfer resistance (R_{ct}) and double-layer capacitance (C_{dl}) of dsDNA + MCH were tested before and after incubation with [Co(GA)$_2$(aqphen)]Cl (200 μM) for 30 minutes.

A typical Nyquist plot for the dsDNA + MCH SAM is shown in Fig. 5 and demonstrates the relative changes in R_{ct} following DNA hybridisation and addition of the [Co(GA)$_2$(aqphen)]Cl complex. DNA hybridisation caused an expected increase in R_{ct} due to an expansion of the electrostatic barrier generated by the negatively charged phosphate groups of the DNA. This expansion reduces the current transferred between the electrode and

solution by increasing charge repulsion to the redox couple ($[Fe(CN)_6]^{3-/4-}$). The average change in R_{ct} upon hybridisation with all samples was 51% (SD: ± 5.1%). This result is similar to the 45% change previously reported in [32] using similar immobilisation conditions but slightly different length oligonucleotides. The $[Co(GA)_2(aqphen)]Cl$ complex caused an additional 15.8% (SD: ± 6.3%) average increase in R_{ct} when incubated with dsDNA + MCH (Fig. 6).

[Figure 5]

Control experiments were performed by incubating the $[Co(GA)_2(aqphen)]Cl$ complex with ssDNA + MCH surfaces and with MCH-only SAMs. Upon incubation with ssDNA + MCH, an average change in R_{ct} of -0.62% (SD: ± 4.2%) was observed. On SAMs with only MCH the average change in R_{ct} after $[Co(GA)_2(aqphen)]Cl$ incubation was -1.8% (± 0.53%). Only negligible changes (< 1%) in C_{dl} were observed throughout all of the conditions (data not shown).

[Figure 6]

3.6. Amperometric responses to the $[Co(GA)_2(aqphen)]Cl$ complex

The redox-activity of the $[Co(GA)_2(aqphen)]Cl$ complex allowed its detection using differential pulse voltammetry (DPV). When $[Co(GA)_2(aqphen)]Cl$ was incubated with ssDNA + MCH or dsDNA + MCH, clear peaks were observed at -0.53 V *vs* $HgSO_4$ reference electrode (Fig. 7). However, the peak areas are 313% larger with dsDNA (peak area: 6.33×10^{-8} AU) than with ssDNA (peak area: 2.02×10^{-8} AU). No peak was observed at a potential range of -0.7 V to 0.3 V (vs $HgSO_4$) when no $[Co(GA)_2(aqphen)]Cl$ had been added to the SAM.

[Figure 7]

4. Conclusions

In this study we have synthesised a novel cobalt compound, $[Co(GA)_2(aqphen)]Cl$, that can enhance DNA detection using both amperometric and impedimetric measurement techniques. EIS measurements have shown an increase in R_{ct} values upon binding of this complex with dsDNA. DPV measurements also demonstrate a clear redox peak when the compound is present and larger peak currents with dsDNA than with ssDNA. Relatively low levels of signal change are observed with non-hybridised DNA but some change is still present and it would be desirable to reduce this. It is likely that some non-specific binding is taking place between the compound and ssDNA, MCH (to a lesser extent) and perhaps on pinholes in the SAM with areas of exposed gold. We can look to reduce non-specific adsorption by modifying the backfill component of the SAM, e.g. by using surface PEGylated SAMs or fouling-resistant 'ternary SAM' systems [33]. The addition of weak detergent molecules, e.g. Tween-20, could also be useful in reducing low level binding of the compound to ssDNA [21].

We intend to look further into the signal enhancement mechanisms of the $[Co(GA)_2(aqphen)]Cl$ complex that creates an increase in charge transfer resistance and redox peak current with dsDNA. It is our current theory that the compound is functioning as a DNA intercalator and so binding would cause structural changes to the DNA that affect the electrostatic barrier. In addition, the compound could be masking the negative charge of the DNA back-bone. These possibilities and others shall be investigated in our future work.

We aim to apply our findings to improving the sensitivity, accuracy and speed of electrochemical DNA detection by using the compound to provide label-free and multi-modal advantages over conventional detection methods. This work could lead to improvements in

point of care testing platforms for testing genetic disorders, pathogen infections and water/food contamination.

Acknowledgements

This work was funded by the SARTRE *Bio-E Initiative* (EPSRC 'Bridging the Gaps'). EMR was sponsored by the UK Ministry of Defence/DSTL. IQS thanks the Kurdistan regional government for funding. We thank Prof. Rudolf K. Allemann (Cardiff University) for access to the Chirascan CD Spectrophotometer.

References

[1] J. Orozco, L.K. Medlin, Review: advances in electrochemical genosensors-based methods for monitoring blooms of toxic algae. *Environ. Sci. Pollut. Res.* (2012) [DOI 10.1007/s11356-012-1258-5]

[2] A. Bonanni, M. Del Valle, Use of nanomaterials for impedimetric DNA sensors: a review. *Anal. Chim. Acta* 678 (2010) 7

[3] W. Vercoutere, M. Akeson, Biosensors for DNA sequence detection. *Curr. Opin. Chem. Biol.* 6 (2002) 816

[4] F. Kuralay, S. Campuzano, D.A. Haake, J. Wang, Highly sensitive disposable nucleic acid biosensors for direct bioelectronic detection in raw biological samples. *Talanta* 85 (2011) 1330

[5] A. Abi, E.E. Ferapontova, Electroanalysis of single-nucleotide polymorphism by hairpin DNA architectures. *Anal. Bioanal. Chem.* 405 (2013) 3693

[6] D. Ozkan, P. Kara, K. Kerman, B. Meric, A. Erdem, F. Jelen, P.E. Nielsen, M. Ozsoz. DNA and PNA sensing on mercury and carbon electrodes by using methylene blue as an electrochemical label. *Bioelectrochemistry* 58 (2002) 119

[7] J. Yang, T. Yang, Y. Feng, K. Jiao, A DNA electrochemical sensor based on nanogold-modified poly-2,6-pyridinedicarboxylic acid film and detection of PAT gene fragment. *Anal. Biochem.* 365 (2007) 24

[8] A. Erdem, K. Kerman, B. Meric, U.S. Akarca, M. Ozsoz. Novel hybridization indicator methylene blue for the electrochemical detection of short DNA sequences related to the hepatitis B virus. *Anal. Chim. Acta* 422 (2000) 139

[9] A. Erdem, M. Ozsoz. Interaction of the anticancer drug epirubicin with DNA. *Anal. Chim. Acta* 437 (2000) 107

[10] A. Erdem, M. Ozsoz, Voltammetry of the anticancer drug mitoxantrone and DNA. *Turk. J. Chem.* 25 (2001) 469

[11] K. Hashimoto, K. Ito, Y. Ishimori, Novel DNA sensor for electrochemical gene detection. *Anal. Chim. Acta* 286 (1994) 219

[12] D.W. Pang, H.D. Abruña, Micromethod for the investigation of the interactions between DNA and redox-active molecules. *Anal. Chem.* 70 (1998) 3162

[13] K.M. Millan, S.R. Mikkelsen, Sequence-selective biosensor for DNA based on electroactive hybridization indicators. *Anal. Chem.* 65 (1993) 2317

[14] M.V. Del Pozo, C. Alonso, F. Pariente, E. Lorenzo, Electrochemical DNA sensing using osmium complexes as hybridization indicators. *Biosens. Bioelectron.* 20 (2005) 1549

[15] P. Kara, D. Ozkan, K. Kerman, B. Meric, A. Erdem, M. Ozsoz. DNA sensing on glassy carbon electrodes by using hemin as the electrochemical hybridization label. *Anal. Bioanal. Chem.* 373 (2002) 710

[16] A. Erdem, B. Meric, K. Kerman, T. Dalbasti, M. Ozsoz, Detection of interaction between metal complex indicator and DNA by using electrochemical biosensor. *Electroanalysis* 11 (1999) 1372

[17] J. Liu, B. Su, G. Lagger, P. Tacchini, H.H. Girault, Antioxidant redox sensors based on DNA modified carbon screen-printed electrodes. *Anal. Chem*. 78 (2006) 6879

[18] A. Erdem, K. Kerman, B. Meric, U.S. Akarca, M. Ozsoz. DNA electrochemical biosensor for the detection of short DNA sequences related to the Hepatitis B virus. *Electroanalysis* 11 (1999) 586

[19] F. Patolsky, A. Lichtenstein, I. Willner, Detection of single-base DNA mutations by enzyme-amplified electronic transduction. *Nat. Biotechnol.* 19 (2001) 253

[20] M. Gebala, L. Stoica, S. Neugebauer, W. Schuhmann. Label-free detection of DNA hybridization in presence of intercalators using electrochemical impedance spectroscopy. *Electroanalysis* 21 (2009) 325

[21] C. Witte, F. Lisdat, Direct detection of DNA and DNA-ligand interaction by impedance spectroscopy. *Electroanalysis* 23 (2011) 339

[22] H.B. Lin, Q.X. Wang, C.M. Zhang, W.Q. Li, Crystal structure and DNA binding studies of a cobalt(II) complex containing mixed-ligands of 1, 10-phenathroline and glycollic acid. *Chin. Chem. Lett.* 22 (2011) 969

[23] R.B. Lopez, B.L. Loeb, T. Boussie, T.J. Meyer, Synthesis of a new phenanthroline derived ligand with acceptor properties. *Tetrahedron Lett.* 37 (1996) 5437.

[24] O. Trott, A.J. Olson, AutoDock Vina: improving the speed and accuracy of docking with a new scoring function, efficient optimization, and multithreading. *J. Comput. Chem.* 31 (2010) 455

[25] M.F. Sanner, B.S. Duncan, C.J. Carrillo, A.J. Olson, Integrating computation and visualization for biomolecular analysis: an example using python and AVS. *Pac. Symp. Biocomput.* (1999) 401

[26] J.E. Jones, A.J. Amoroso, I.M. Dorin, G. Parigi, B.D. Ward, N.J. Buurma, S.J.A. Pope, Bimodal, dimetallic lanthanide complexes that bind to DNA: the nature of binding and its influence on water relaxivity. *Chem. Commun.* 47 (2011) 3374

[27] E.F. Pettersen, T.D. Goddard, C.C. Huang, G.S. Couch, D.M. Greenblatt, E.C. Meng, T.E. Ferrin, UCSF Chimera--a visualization system for exploratory research and analysis. *J. Comput. Chem.* 25 (2004) 1605

[28] M.W. Schmidt, K.K. Baldridge, J.A. Boatz, S.T. Elbert, M.S. Gordon, J.H. Jensen, S. Koseki, N. Matsunaga, K.A. Nguyen, S. Su, T.L. Windus, M. Dupuis, J.A. Montgomery Jr, General atomic and molecular electronic structure system. *J. Comput. Chem.* 14 (1993) 1347

[29] Y. Zhao, D.G. Truhlar, The M06 suite of density functionals for main group thermochemistry, thermochemical kinetics, noncovalent interactions, excited states, and transition elements: two new functionals and systematic testing of four M06-class functionals and 12 other functionals. *Theor. Chem. Account* 120 (2008) 215

[30] K.P. Jensen, J. Cirera, Accurate computed enthalpies of spin crossover in iron and cobalt complexes. *J. Phys. Chem. A* 113 (2009) 10033

[31] R. Lopez, A.M. Leiva, F. Zuloaga, B. Loeb, E. Norambuena, K.M. Omberg, J.R. Schoonover, D. Striplin, M. Devenney, T.J. Meyer, Excited-state electron transfer in a

chromophore-quencher complex: spectroscopic identification of a redox-separated state. *Inorg. Chem.* 38 (1999) 2924

[32] S.D. Keighley, P. Li, P. Estrela, P. Migliorato, Optimization of DNA immobilization on gold electrodes for label-free detection by electrochemical impedance spectroscopy. *Biosens Bioelectron.* 23 (2008) 1291

[33] S. Campuzano, F. Kuralay, M.J. Lobo-Castañón, M. Bartošík, K. Vyavahare, E. Paleček, D.A. Haake, J. Wang, Ternary monolayers as DNA recognition interfaces for direct and sensitive electrochemical detection in untreated clinical samples. *Biosens Bioelectron.* 26 (2011) 3577

Figure captions

Figure 1: Synthetic route to the cobalt complex. (i) EtOH, heat; (ii) EtOH, 1 eq. $CoCl_2.6H_2O$, 2 eq. glycolic acid / NaOH(aq).

Figure 2: Top 3 docked poses for $Co(GA)_2$(aqphen) interacting with open-d(ATCGAGA**CG**TCTCGAT)$_2$

Figure 3: Cyclic voltammogram of [$Co(GA)_2$(aqphen)]Cl in DMF at a scan rate of 200 mVs^{-1}.

Figure 4: Absorbance at 394 nm for a solution of 41.7 μM $Co(GA)_2$(aqphen) upon addition of fish sperm DNA in the concentration range $0-255$ μM in deionised water at 25 °C (DNA concentrations are concentrations of base pairs). The solid line represents the best fit of the multiple independent binding sites model to the second part of the data. The inset shows the average absorbance between 550 nm and 600 nm for a solution of 41.7 μM $Co(GA)_2$(aqphen) upon addition of fish sperm DNA in the concentration range $0-56.3$ μM in deionised water at 25 °C, error bars represent the standard deviation in the absorbance between 550 nm and 600 nm.

Figure 5: A representative Nyquist plot showing responses to DNA hybridisation and [$Co(GA)_2$(aqphen)]Cl. The percent changes in charge transfer resistance (R_{ct}) after DNA hybridisation and [$Co(GA)_2$(aqphen)]Cl incubation are shown below the arrows.

Figure 6: The effect of [$Co(GA)_2$(aqphen)]Cl on charge transfer resistance (R_{ct}). Data are shown for (1) MCH, (2) ssDNA + MCH and (3) dsDNA + MCH. Error bars represent standard deviations of mean values determined from three individual experiments (n = 3).

Figure 7: Differential pulse voltammograms showing [$Co(GA)_2$(aqphen)]Cl responses to DNA/MCH-functionalised gold electrodes. Data are shown for (1) ssDNA/MCH,

(2) ssDNA/MCH + $[Co(GA)_2(aqphen)]Cl$ and (3) dsDNA/MCH + $[Co(GA)_2(aqphen)]Cl$. DPV measurements were done in 100 mM PB (pH 7.4). The data were normalised by subtracting the background baseline using fitting software.

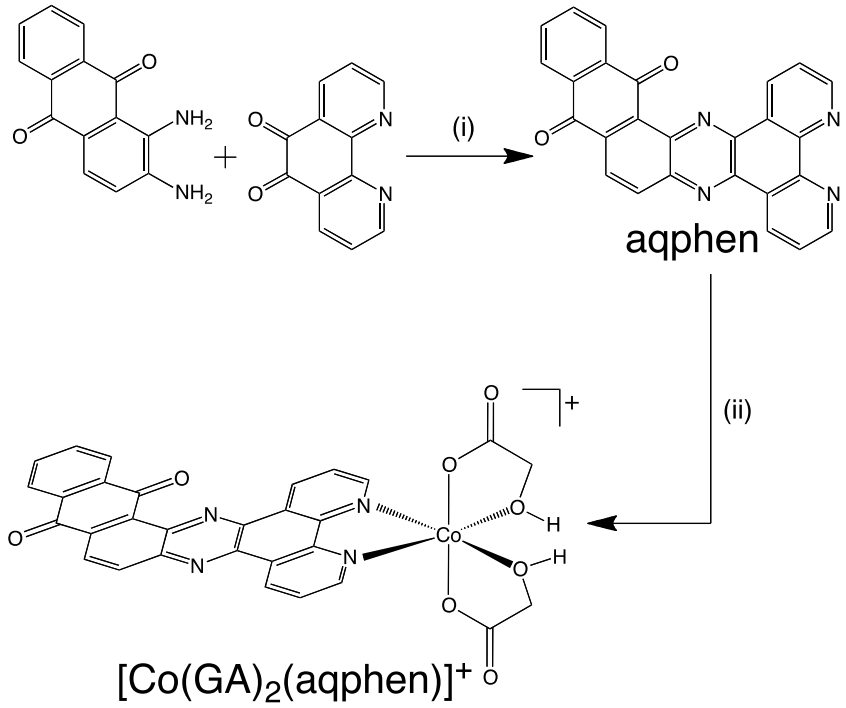

Figure 1: Synthetic route to the cobalt complex. (i) EtOH, heat; (ii) EtOH, 1 eq. $CoCl_2.6H_2O$, 2 eq. glycollic acid / NaOH(aq).

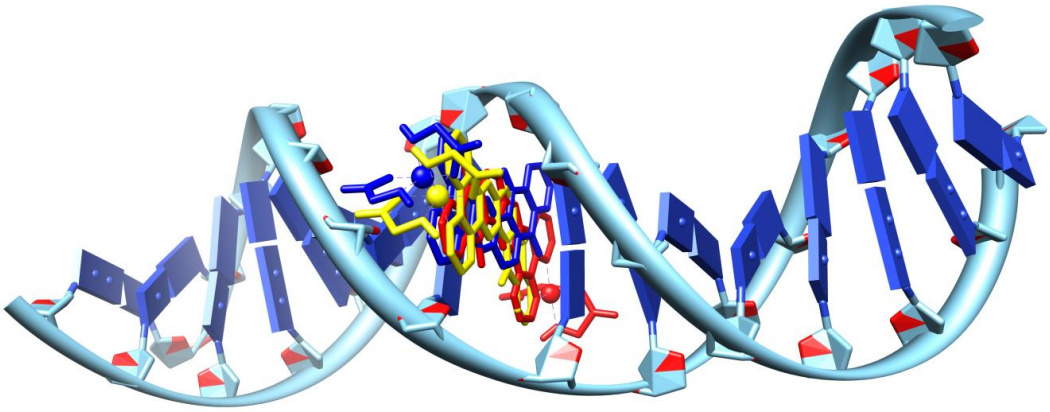

Figure 2: Top 3 docked poses for $Co(GA)_2(aqphen)$ interacting with open-d(ATCGAGA**CG**TCTCGAT)$_2$

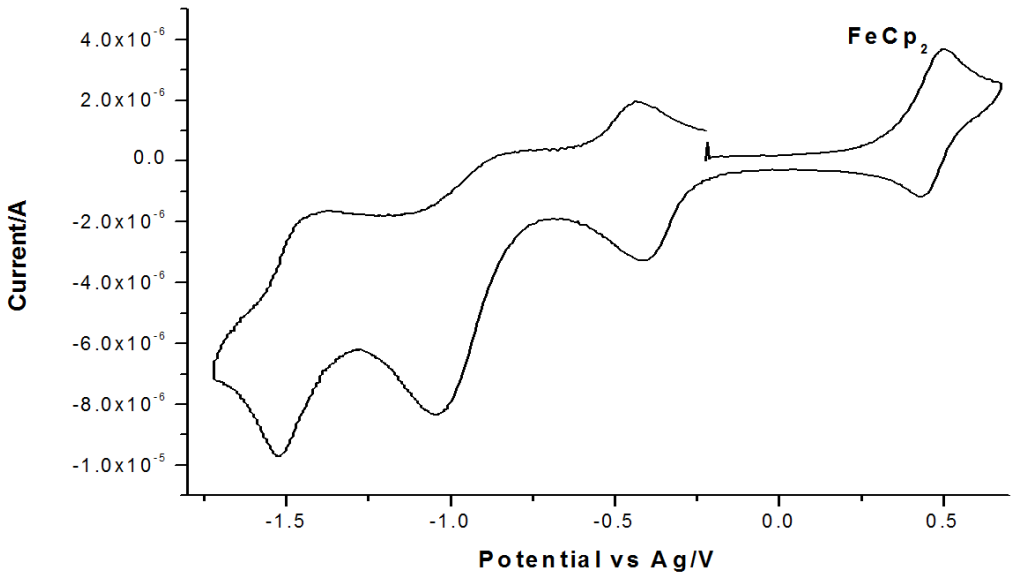

Figure 3: Cyclic voltammogram of $[Co(GA)_2(aqphen)]Cl$ in DMF at a scan rate of 200 mVs^{-1}.

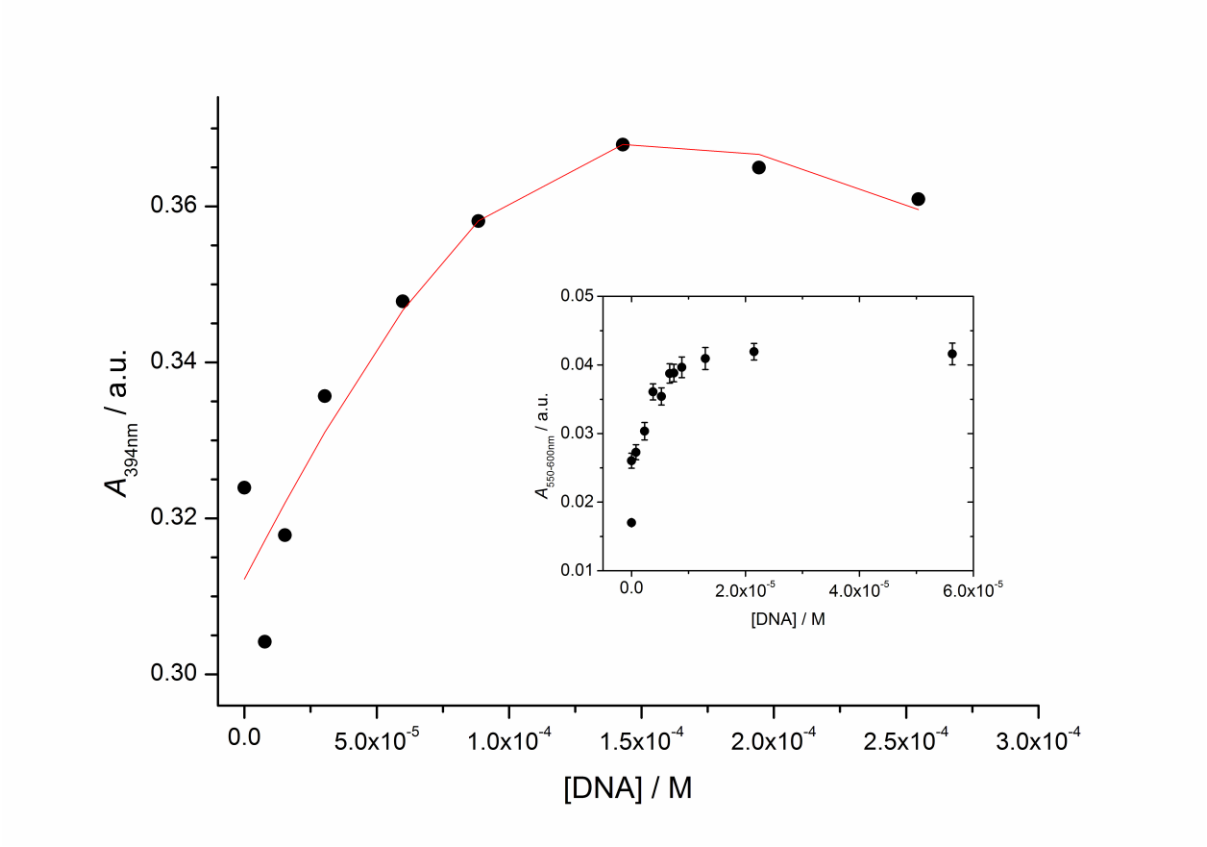

Figure 4: Absorbance at 394 nm for a solution of 41.7 μM $Co(GA)_2(aqphen)$ upon addition of fish sperm DNA in the concentration range 0 – 255 μM in deionised water at 25 °C (DNA concentrations are concentrations of base pairs). The solid line represents the best fit of the multiple independent binding sites model to the second part of the data. The inset shows the observed increase in average absorbance between 550 nm and 600 nm for a solution of 41.7 μM $Co(GA)_2(aqphen)$ upon addition of fish sperm DNA in the concentration range 0 – 56.3 μM in deionised water at 25 °C, error bars represent the standard deviation in the absorbance between 550 nm and 600 nm.

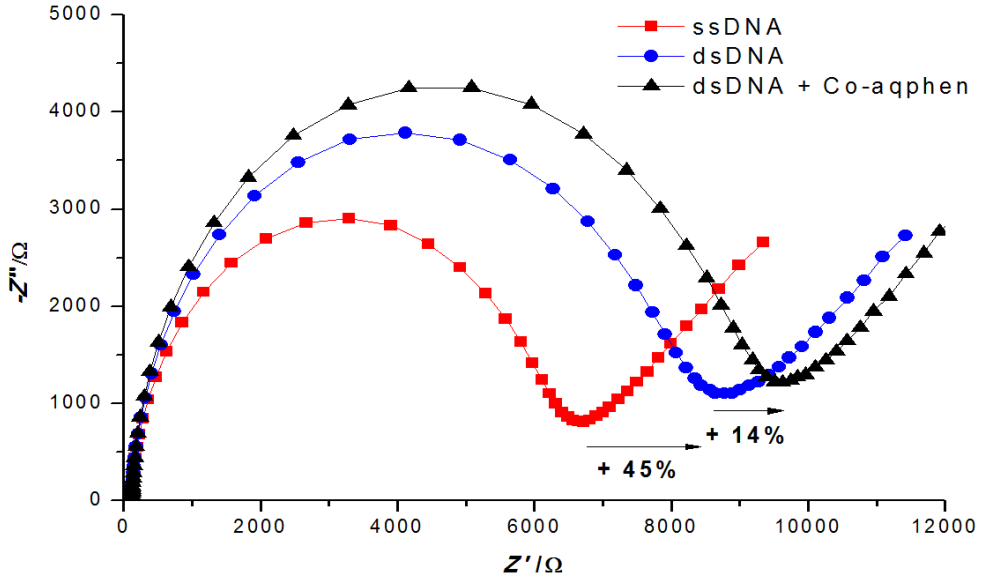

Figure 5: A representative Nyquist plot showing responses to DNA hybridisation and $[Co(GA)_2(aqphen)]Cl$. The percent changes in charge transfer resistance (R_{ct}) after DNA hybridisation and $[Co(GA)_2(aqphen)]Cl$ incubation are shown below the arrows.

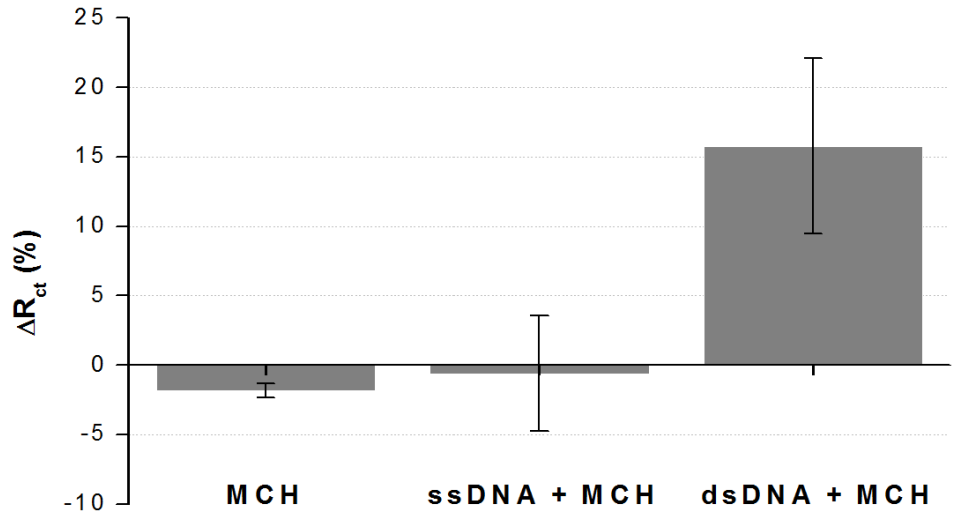

Figure 6: The effect of $[Co(GA)_2(aqphen)]Cl$ on charge transfer resistance (R_{ct}). Data are shown for (1) MCH, (2) ssDNA + MCH and (3) dsDNA + MCH. Error bars represent standard deviations of mean values determined from three individual experiments (*n* = 3).

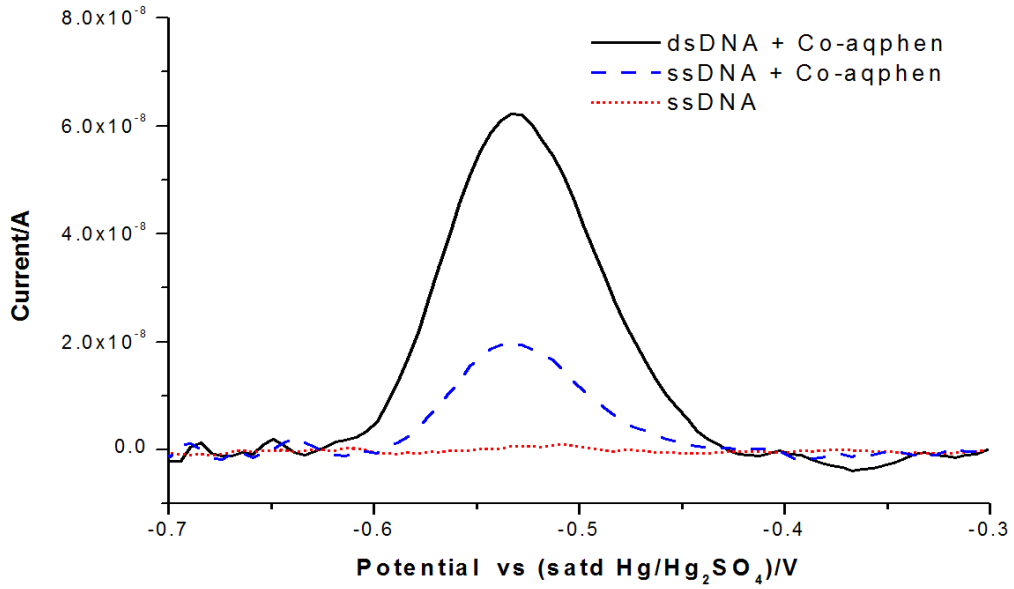

Figure 7: Differential pulse voltammograms showing $[Co(GA)_2(aqphen)]Cl$ responses to DNA/MCH-functionalised gold electrodes. Data are shown for (1) ssDNA/MCH, (2) ssDNA/MCH + $[Co(GA)_2(aqphen)]Cl$ and (3) dsDNA/MCH + $[Co(GA)_2(aqphen)]Cl$. DPV measurements were done in 100 mM PB (pH 7.4). The data were normalised by subtracting the background baseline using fitting software.